Atmos. Chem. Phys., 15, 8751–8765, 2015
www.atmos-chem-phys.net/15/8751/2015/
doi:10.5194/acp-15-8751-2015

Atmospheric Chemistry and Physics
Open Access

Trace metal characterization of aerosol particles and cloud water during HCCT 2010

K. W. Fomba[1], D. van Pinxteren[1], K. Müller[1], Y. Iinuma[1], T. Lee[2,a], J. L. Collett Jr.[2], and H. Herrmann[1]

[1]Leibniz-Institute for Tropospheric Research (TROPOS), Permoserstr. 15, 04318 Leipzig, Germany
[2]Department of Atmospheric Science, Colorado State University, Ft. Collins, CO 80523, USA
[a]now at: Hankuk University of Foreign Studies, Department of Environmental Sciences, Yongin, South Korea

Correspondence to: H. Herrmann (herrmann@tropos.de)

Received: 6 March 2015 – Published in Atmos. Chem. Phys. Discuss.: 14 April 2015
Revised: 9 July 2015 – Accepted: 19 July 2015 – Published: 10 August 2015

Abstract. Trace metal characterization of bulk and size-resolved aerosol and cloud water samples were performed during the Hill Cap Cloud Thuringia (HCCT) campaign. Cloud water was collected at the top of Mt. Schmücke while aerosol samples were collected at two stations upwind and downwind of Mt. Schmücke. Fourteen trace metals including Ti, V, Fe, Mn, Co, Zn, Ni, Cu, As, Sr, Rb, Pb, Cr, and Se were investigated during four full cloud events (FCEs) that fulfilled the conditions of a continuous air mass flow through the three stations. Aerosol particle trace metal concentrations were found to be lower than those observed in the same region during previous field experiments but were within a similar range to those observed in other rural regions in Europe. Fe and Zn were the most abundant elements with concentration ranges of 0.2–111.6 and 1.1–32.1 ng m^{-3}, respectively. Fe, Mn, and Ti were mainly found in coarse mode aerosols while Zn, Pb, and As were mostly found in the fine mode. Correlation and enrichment factor analysis of trace metals revealed that trace metals such as Ti and Rb were mostly of crustal origin while trace metals such as Zn, Pb, As, Cr, Ni, V, and Cu were of anthropogenic origin. Trace metals such as Fe and Mn were of mixed origins including crustal and combustion sources. Trace metal cloud water concentration decreased from Ti, Mn, Cr, to Co with average concentrations of 9.18, 5.59, 5.54, and 0.46 µg L^{-1}, respectively. A non-uniform distribution of soluble Fe, Cu, and Mn was observed across the cloud drop sizes. Soluble Fe and Cu were found mainly in cloud droplets with diameters between 16 and 22 µm, while Mn was found mostly in larger drops greater than 22 µm. Fe(III) was the main form of soluble Fe especially in the small and larger drops with concentrations ranging from 2.2 to 37.1 µg L^{-1}. In contrast to other studies, Fe(II) was observed mainly in the evening hours, implying its presence was not directly related to photochemical processes. Aerosol–cloud interaction did not lead to a marked increase in soluble trace metal concentrations; rather it led to differences in the chemical composition of the aerosol due to preferential loss of aerosol particles through physical processes including cloud drop deposition to vegetative surfaces.

1 Introduction

Aerosol trace metals play important roles in aerosol–cloud interactions as they can serve as good catalysts for aqueous-phase reactions. They are useful in understanding chemical processes and in the identification of parameters that are important in controlling aerosol behavior. Dissolved trace metals can form complexes with water, sulfate, and organic compounds and can thereby influence their redox cycles (Zuo and Hoigne, 1994; Jacob and Hoffmann, 1983). They play important roles in the oxidation of S (IV) to S (VI), which has been shown to substantially influence the sulfate budget and thus the formation of cloud droplets (Harris et al., 2013). Transition metal ions such as iron and copper significantly influence the OH radical budget in aqueous media as they can react efficiently with many oxidizing and reducing agents such as HO_2 / O_2 radicals and hydrogen peroxide in aqueous media (Deguillaume et al., 2005; Spokes et al., 1994). On the other hand, photochemical dissociation of metal complexes may also lead to sources of OH radicals and hydrogen peroxide. Trace metals, therefore, play important roles in the

variation of the oxidative capacity of the atmosphere (Deguillaume et al., 2005; Spokes et al., 1994). Nevertheless, their reactivity is closely related to their concentrations in aqueous media (Clarke and Radojevic, 1987). To assess the importance and further understand the various reactions that are influenced by trace metals, it is necessary to quantify their concentrations in cloud drops and aerosol particles.

Trace metals in continental aerosols originate from extremely complex mixtures of gaseous and particulate components comprising of motor vehicle emissions, abrasion of tires or brake linings, road dust, fly ashes from wood, coal, lignite and oil combustion, refuse incineration, and also crustal weathering. This mixture influences the chemical composition and properties of the aerosol as well as the state at which trace metals are available in the aerosol particles. Depending on the location and meteorological conditions, the sources of trace metals can differ significantly, leading to variations in the trace metal and chemical composition of the aerosol. Trace metal concentrations vary according to their sources. Crustal sources are usually found to strongly influence concentrations of trace metals such as Fe, Al, Ti, and Mn with concentration ranges of up to a few $\mu g\,m^{-3}$, especially during dust storms. However, in rural and continental background regions, trace metal concentrations are relatively lower. In cloud water a wide range of concentrations has been observed (Deguillaume et al., 2005) which has also been found to influence the chemical reactions they take part in, as well as the composition of the aerosol after cloud processing. During the past years some studies have reported trace metal concentrations in different cloud conditions during various field measurements (Plessow et al., 2001; Cini et al., 2002; Hutchings et al., 2009; Mancinelli et al., 2005; Burkhard et al., 1992; Siefert et al., 1998; Liu et al., 2012; Bruggemann et al., 2005; Wang et al., 2014; Straub et al., 2012; Li et al., 2013; Guo et al., 2012; Rao and Collett, 1998) showing strong variability due to the location and air mass history.

During the Hill Cap Cloud Thuringia (HCCT) experiment that took place in autumn 2010, trace metals were characterized both in aerosol particles at two valley stations, upwind of and downwind from the Schmücke mountain, as well as in cloud water collected at the top of the mountain. The aim was to characterize the trace metal content in the aerosol before and after the particles interact with the cloud and also in cloud water in order to investigate the role of trace metals in altering the chemical composition of the cloud and the properties of the particles after passing through the cloud. Four full cloud events (FCEs) during which the air mass was found to have traveled through all three stations and the strict criteria of the experiment were fulfilled as described in Tilgner et al. (2014) were chosen. In this study the temporal variation of the trace metals during the selected FCEs and the changes in trace metal particle size distribution and their properties after the passage of the particles through the cloud will be presented.

2 Experimental setup

2.1 Sampling site

The HCCT-2010 experiment was carried out in the Thüringer Wald, Germany. Based on the experience from the previous FEBUKO (Herrmann et al., 2005) field studies at the same site, sampling was done in the months of September and October in 2010. Three measurement stations were built. One in-cloud mountain station, Mt. Schmücke, and two valley stations, Goldlauter (GL; upwind of the summit station) and Gehlberg (GB; downwind of the summit station) were set up. Cloud water collection was carried out only at Mt. Schmücke while aerosol particle sampling was conducted at the valley stations. A detailed description of the experiment, sampling site, and meteorological conditions during the experiment has been reported by Tilgner et al. (2014).

2.2 Aerosol sampling

Size-resolved aerosol particle sampling was conducted using a humidity controlled low-pressure five-stage Berner impactor with a PM_{10} cutoff. The collected particle diameter ranged from 0.05 to 10 µm with lower stage cutoffs (stages 1 to 5) at aerodynamic diameters of 0.05, 0.14, 0.42, 1.2, and 3.5 µm. For the regulation of the humidity, seven parallel tubes were used after the isokinetic inlet to regulate the relative humidity to approx. 80 % via heating/cooling of the tubes. This was done in order to avoid water condensation on the impaction substrates under very humid conditions during cloud appearance at Mt. Schmücke and particle bounceoff during very dry condition. The impactors were operated with aluminum foils and polycarbonate foils placed upon them as impaction substrates. The aluminum foils were used for aerosol mass, organic / elemental carbon (OC / EC) and inorganic ions as well as levoglucosan analysis, while the polycarbonate foils were used for trace metal analysis. Bulk particulate matter sampling was completed on Munktell quartz fiber filters using a high-volume sampler (Digitel DHA-80) with a PM_{10} inlet. The inlet height of the collectors was 4 m above ground level.

2.3 Cloud water sampling

Bulk cloud water was collected using four stainless steel compact Caltech Active Strand Cloudwater Collectors (CASCC2) (Demoz et al., 1996). As will be further discussed below, due to the utilization of the stainless steel collector, high blanks of some trace metals were observed. For size-resolved cloud water collection, a three-stage plastic CASCC (Raja et al., 2008) cloud water collector with nominal cloud droplet cutoffs (50 % lower cut size specified as drop diameter) at 4, 16, and 22 µm was used. Bulk cloud water samples were collected every hour, while size-resolved samples were taken at a 2 h time resolution during cloud events. Aliquots were taken immediately after sample collection for on-site

analysis or stabilization of trace species, and the remainders of the sample volumes were frozen. For soluble trace metal redox state analysis, which was completed immediately after collection of the samples at the sampling site, 1 mL cloud water was filtered through a 0.45 µm syringe filter and 0.5 mL filtrate was obtained for the analysis.

2.4 Chemical analysis

Total trace metal analysis was performed using total reflection X-ray fluorescence (TXRF) analysis. Size-resolved trace metals were analyzed from the polycarbonate foils that were placed on the aluminum foils on each impactor stage. Only filters from impactor stages 1 to 4 were used for trace metal analysis since impaction spots on the fifth stage were mostly not visible. Thus, the trace metal concentration at the valley stations is representative of $PM_{3.5}$. For TXRF analysis, the impacted spots on the polycarbonate foils were cut and placed on a TXRF carrier and were spiked with conc. HNO_3 and Ga (as an internal standard) and subsequently left to evaporate at 100 °C. The carrier was thereafter cooled to room temperature and measured. Blank filters that were loaded in the impactor, with no air sucked through them, were also analyzed using the same procedure as the sampled filters. Further details of the sample preparation procedure as well as the limitations of this method have been previously described (Fomba et al., 2013). The analyzed aerosol trace metals were Ti, V, Cr, Mn, Fe, Co, Ni, Cu, Zn, Se, Pb, As, Rb, and Sr. Trace metal blank correction for the aerosol samples was performed by subtracting the elemental average concentrations of the blank filters from each analyzed sample. Due to this procedure, values for trace metals with low concentrations ($< 0.01\,ng\,m^{-3}$) especially for the fine mode particles in stages 1 and 2 were accompanied with uncertainties of about 15 % especially for metals such as V, As, and Sr. PM_{10}-soluble aerosol trace metals were also analyzed using TXRF from 0.45 µm syringe filtrates of PM_{10} filters extracted in deionized (DI) water. The extracts were filtered in order to eliminate the contribution of particulate matter to the measured soluble concentrations.

For cloud water analysis, aliquots were spiked with 69 % conc. HNO_3 solution and heated in a water bath at 60 °C for 4 h. After cooling, aliquots of 100 µL were taken and brought onto the TXRF carrier surface via pipetting (4×25 µL). Ga was then added to the sample to serve as internal standard for the TXRF measurements. These analyses could not be performed on size-resolved cloud water samples due to insufficient sample volume and were thus performed only on bulk cloud water samples. For the bulk cloud water samples only Ti, V, Cr, Mn, Co, Se, Pb, As, Rb, and Sr were analyzed. Fe, Ni, Cu, and Zn were excluded from the analysis due to contamination arising from sample collection and preparation. For the analysis of OC / EC, inorganic ions, and levoglucosan, the same procedure as described earlier (Müller et al., 2010; Iinuma et al., 2007) was used.

Cloud water trace metal blanks were measured from blank samples that were collected after cleaning of the stainless steel bulk cloud water collector with deionized water after each cloud event. The blanks were not subtracted since they were considered to be influenced by residual materials in the collectors from previous cloud events that were not fully removed during the cleaning process. Therefore, the first collected sample of each event was not considered in the data analysis due to likely strong influence of the wash-off of the collectors. However, most trace metal blanks were lower than 25 % of the hourly cloud water concentrations except for Fe, Cu, Ni, and Zn, whose blanks were mostly higher (up to 65 %) than the hourly concentrations. The results of these four trace metals were thus considered to be very inaccurate and were, therefore, not considered in the further analysis of the results.

For the analyses of the soluble transition metal ions (TMIs) redox states, a DIONEX ICS 900 ion chromatography instrument, equipped with a CS5A column and a UV–VIS detector was used. Using this instrument, transition metal ions such as Fe(III), Fe(II), Cu(II), and Mn(II) can be determined via post-column derivatization simultaneously. This is performed via a procedure similar to the one reported by Oktavia et al. (2008), however using a 4-(2-pyridylazo) resorcinol (PAR, P/N 039672) as post-column reagent. This combination renders a good separation of the abovementioned ions making the analysis easier to handle. TMI redox state measurements were only performed on size-resolved cloud water samples. As indicated above, similar redox state measurements on bulk cloud water samples were not considered for the data interpretation due to their high blank values.

3 Results and discussion

The presented results are focused on data obtained during four FCEs): FCE 1.1 (14 September 2010 11:00 to 15 September 2010, 02:00), FCE 11.3 (2 October 2010, 14:30 to 19:30), FCE 13.3 (6 October 2010, 12:15 to 7 October 2010, 03:15), and FCE 22.1 (19 October 2010, 21:30 to 20 October 2010, 03:30). All times in the manuscript are given in CEST (Central European Summer Time). The results will be presented in two sections. The first section will focus on the aerosol particle analysis and the second on cloud water analysis.

3.1 Aerosol trace metal concentrations

The aerosol trace metal concentrations during HCCT-2010 at the valley stations are presented in Table 1. Reported trace metal concentrations in other rural regions in Europe and during previous experiments in this region reported by Rüd (2003) are also presented in Table 1 for comparison. Amongst the 14 investigated elements, Fe was the most abun-

Table 1. Aerosol trace metal concentration averages ± standard deviation and ranges during HCCT at the valley stations and results from the FEBUKO experiment by Rüd (2003): Ref 1 and other studies. Ref 2: G. Boccadifalco, Italy (Dongarra et al., 2010); Ref 3, 4: Auchencorth, Castlemorton, UK (Allen et al., 2001); Ref 5 and 6; Payerne and Chaumont, Switzerland (Hueglin et al., 2005); Ref 7: Venice, Italy (Masiol et al., 2015); Ref 8: Puy de Dôme, France (Vlastelic et al., 2014); Ref 9: K-Puska, Hungary (Maenhaut et al., 2008); Ref 10: Hyytiälä, Finland (Maenhaut et al., 2011); Ref 11: Diabla Gora, Poland (Rogula-Kozlowska et al., 2014); Ref 12: Bertiz, Spain (Aldabe et al., 2011); Ref 13: Monte Cimone, Italy (Marenco et al., 2006); Ref 14: Monte Martano, Italy (Moroni et al., 2015).

Elements			Ti	V	Cr	Mn	Co	Fe	Ni	Cu	Zn	Se	Pb	As	Rb	Sr
HCCT-2010	$PM_{3.5}$	Mean ± SD	0.9 ± 0.9	0.18 ± 0.1	2.7 ± 4.3	0.4 ± 0.5	0.02 ± 0.03	16.5 ± 21.2	0.38 ± 0.7	0.7 ± 0.44	11.1 ± 7.6	0.57 ± 0.9	1.3 ± 0.7	0.28 ± 0.3	0.04 ± 0.03	0.43 ± 0.3
		Range	0.04–3.9	0.03–0.4	0.35–21.9	0.01–2.4	0.01–0.11	0.22–111.6	0.02–2.5	0.10–2.19	1.1–32.1	0.02–3.7	0.25–2.9	0.01–1.21	0.01–0.1	0.02–1.7
Ref 1	$PM_{2.5}$	Mean ± SD	9.6 ± 10		1.0 ± 1.4	1.8 ± 1.4	0.1 ± 0.1	97 ± 60	6.1 ± 3.3	7.2 ± 3.1	9.2 ± 4.7		5.6 ± 2.0	0.2 ± 0.1		1. ± 0.8
		Range	1.9–29		0.1–3.5	0.02–5.0	0.01–0.3	14–218	2.4–12	1.2–13	5.9–16		2.5–10	0.04–0.4		0.03–2.9
Ref 2	TSP	Mean ± SD				1.5 ± 1.2			0.8 ± 1.3	1.1 ± 1.2	5.2 ± 1.2		10 ± 1.9			0.41 ± 1
Ref 3	TSP	Mean ± SD				1.7 ± 2.1	0.06 ± 1.4	78 ± 2.5	1.3 ± 1.8	1.1 ± 2.2	11 ± 2	1.1 ± 1.3	7.9 ± 2.2			0.71 ± 1.4
Ref 4	PM_{10}	Mean		0.7		2.8		89	1.2	6		0.16	10	0.53	0.3	
Ref 5	$PM_{2.5}$	Mean		0.8		0.8		26	1.3	6		0.2	4.7	0.16	0.15	
Ref 6	PM_{10}	Mean		2.6	0.5	4.6		340		17	18		8.2			
		Range		1.2–4.8	10–28	0.7–7		102–1152		6–58	6.2–41	< 14	2.8–23	< 2.3		
Ref 7	PM_1	Mean	3.1	3.1	5.9	6.8		66.5	3	3.8	38.8					
	1 to 4	Mean	9.2	0.2	3.2	3.1		53.7	12.6	27.2	49.8					
	$PM_{>4}$	Mean	8.3		10.1	0.7		12.7	1.1	1.3	3.2					
Ref 8	PM_{10}	Mean ± SD	6 ± 10	0.2 ± 0.3	1.6 ± 4.7	2.3 ± 3.8	0.05 ± 0.08	62 ± 89	1.9 ± 4.2	5.8 ± 22.1	9.4 ± 15.2	0.02 ± 0.03	1.3 ± 4.4	0.05 ± 0.06	0.16 ± 0.23	0.55 ± 0.79
Ref 9	PM_{10}	Median	4.4			2.6		86		1.93	10		4			
		IQR	3.2–6.0			2.1–4.0		59–137		1.58–3.2	8–18.3		3.2–6.0			
Ref 10	$PM_{2.5}$	Median	0.92			0.52		17.1	0.5	0.34	6		1.59			
	PM_{10}	Median	5.7			2		67	0.44	0.67	6.7		1.45			
		IQR	2.4–8.4			1.2–2.9		46–98	0.28–0.6	0.38–1.0	2.8–10.3		0.65–3.0			
Ref 11	$PM_{2.5}$	Mean range							0.4–1.1				2.3–13.7	0.2–0.6		
Ref 12	PM_{10}	Mean	11.26		1.3	2.2	0.12	0.09	0.9	2.03	17.3	0.27	2.88	0.1	0.58	1.2
		Range	3.9–80.9		< 10.9	< 18.2	< 0.01–1.1	< 0.01–0.7	0.01–21.8	< 8.1	3.0–79.5	0.1–0.6	< 11.6	< 0.01–0.7	0.16–2.1	< 0.01–5.1
Ref 13	PM_{10}	Mean ± SD	30 ± 50	3.1 ± 1.5		6.2 ± 7		260 ± 440	1.4 ± 0.5	2.9 ± 3.1	9.9 ± 6		3.9 ± 2.4			2.7 ± 2.8
Ref 14	$PM_{2.5}$	Mean ± SD	2.0 ± 1.6		1.8 ± 0.85	0.7 ± 0.5		48 ± 44	0.5 ± 0.18	5.0 ± 1.0	5.9 ± 3.3		1.7 ± 0.27			

IQR is inter-quartile ranges; all concentrations are in ng m^{-3}.

dant element. Similar findings were obtained by Rüd (2003) during the FEBUKO experiment. The next most abundant trace metals were Zn, Cr, and Pb. Iron concentrations were within the range of 0.2–111.6 ng m^{-3} with an average value of 16.5 ng m^{-3} while Zn, Cr, and Pb values were within the ranges of 1.1–32.1, 0.4–21.9, and 0.3–2.9 ng m^{-3} with average values of 11.1, 2.7, and 1.3 ng m^{-3}, respectively. The average aerosol particle mass concentrations of the other elements were all less than 1 ng m^{-3}, but their concentrations ranged between 0.01 and 4 ng m^{-3}. The concentration ranges of elements such as Cr, Mn, and Zn were within the same order of magnitude as those reported by Rüd (2003) during the FEBUKO campaign in the same location. Comparatively, the mean concentrations and the obtained concentration ranges during HCCT-2010 were in good agreement with those reported at other rural regions in Europe. For trace metals such as Cr and Zn, their mean concentrations were higher than those reported at Boccadifalco, Italy (Dongarra et al., 2010), Puy de Dôme, France (Vlastelic et al., 2014), K-Puska, Hungary (Maenhaut et al., 2008), Monte Cimone, Italy (Marenco et al., 2006) Monte Martano, Italy (Moroni et al., 2015), and at Auchencorth (UK) (Allen et al., 2001); however, in the case of Zn the average concentration was comparable with that observed at Castlemorton (UK) (Allen et al., 2001) but lower than that reported at the Schmücke (Rüd, 2003) and at Bertiz, Spain (Aldabe et al., 2011). However, the concentration ranges were similar to those reported by Rüd (2003). Trace metals such as Sr and As showed comparable average values and ranges to those reported at other rural sites in Italy (Dongarra et al., 2010; Allen et al., 2001; Hueglin et al., 2005), UK, and Switzerland as well as at Bertiz, Spain (Aldabe et al., 2011), and Diabla Gora, Poland (Rogula-Kozlowska et al., 2014).

Se and Rb mean concentrations were lower than those reported at Bertiz, Spain (Aldabe et al., 2011), and Puy de Dôme, France (Vlastelic et al., 2014). For trace metals such as Ti, Co, Fe, Ni, Cu, and Pb, the mean concentrations were lower than those reported in the above-stated sites except for Fe and Cu which were higher than the values reported at Bertiz, Spain (Aldabe et al., 2011), and at Hyytiälä, Finland (Maenhaut et al., 2011), respectively. However, the concentration ranges of these metals were within the same order of magnitude as those reported at the other rural sites. The lower average values obtained during HCCT-2010 than those reported at other rural sites are likely due to the different geographical settings of the sampling sites and the different particulate matter size ranges sampled at some of these sites. The measurements at the UK sites were based on total suspended particulate matter (TSP) while the measurements at Payerne in Switzerland (Hueglin et al., 2005) and the measurements from Rüd (2003), Puy de Dôme (Vlastelic et al., 2014), and K-Puska (Maenhaut et al., 2008) were done on PM_{10} particles and those during HCCT-2010 on $PM_{3.5}$ particles. In addition, Goldlauter and Gehlberg do not experience frequent strong air mass outflow from major urban cities as do the other investigated sites. The differences in the observed concentrations between HCCT-2010 and those reported by Rüd (2003) during the FEBUKO experiment could also be due to a reduction in particulate matter emission in Germany and central Europe during the past 15 years. It has been observed in other rural regions in Germany that the PM_{10} concentration has dropped by more than 10 % within the past decade (Spindler et al., 2013). Although these values varied during the campaign as shown in their ranges, their size distributions were different as the air mass parcel crossed the mountain station to the downwind station.

3.2 Aerosol trace metal size distribution

Figure 1 shows the size distribution of the trace metals during four full cloud events (FCE 1.1, FCE 11.3, FCE 13.3, and FCE 22.1). In principle, the aerosol mass may decrease during the passage of the air mass parcel through the cloud and over the mountain due to particle and/or cloud droplet deposition during air mass transit across the forested mountain. Entrainment of cleaner air from above might also reduce concentrations or, in the case of more polluted air mass from above, increases the concentration. However, during HCCT, the meteorological analysis as reported by Tilgner et al. (2014) did not show strong entrainment from more polluted air masses especially during the selected events. In Fig. 1, such a trend is observed for FCEs 1.1, 13.3, and 22.1 wherein the total trace metal mass decreased from the upwind side (GL) to the downwind side (GB) of the mountain. During FCE 11.3, there was no significant difference in the total particle trace metal mass, suggesting there may have been limited deposition or an influence from local sources such as traffic, as seen in the increase in the Cr, Cu, and Ni concentrations. During FCE 1.1 Fe was mostly found in the coarse mode, while Zn and Pb were mostly found in the fine modes (stages 2 and 1) at Goldlauter. In Gehlberg, the trace metal size distribution changed with the trace metals concentrated in the fine mode as compared to the coarse mode observed in Goldlauter. The different concentrations and size distributions are indicative of preferential particle loss during this event as a significant part of the concentration difference is largely due to the decrease in the Fe concentration by a factor of 4 in the fourth stage. The decrease in the mass concentration is related to loss of Fe-containing material after passage of the air mass through the cloud, especially as iron is mostly found in the coarse mode. Coarse mode particles are usually emitted from mechanical processes such as resuspension of soil particles in the atmosphere or abrasion of car parts due to friction or from other industrial processes. These particles are larger and heavier and can therefore be easily lost through deposition.

During FCE 11.3 the size distribution did not vary largely. Although a decrease in the fine mode fraction was apparent especially due to loss of Zn- and Pb-containing particles, the changes in the coarse mode fraction were not significant. Cr,

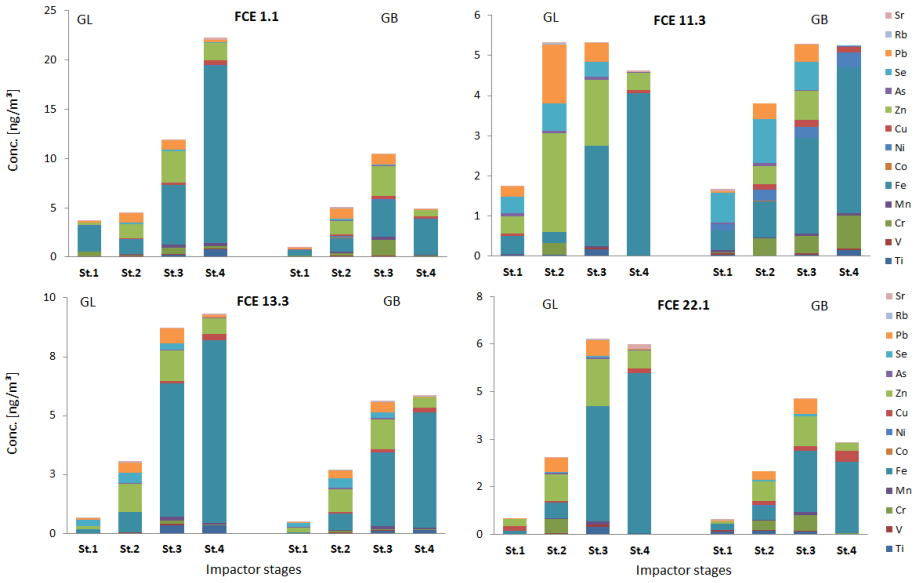

Figure 1. Aerosol particle size-resolved trace metal concentrations during four full cloud events at Goldlauter (GL) and Gehlberg (GB). The PM stage cutoffs for St. 1 to St. 4 are 0.05, 0.14, 0.42, 1.2, and 3.5 µm, respectively.

Cu, and Ni concentrations were found to be higher at GB. Although entrainment of more polluted air masses may lead to an increase in the concentration of trace metals in the downwind site, meteorological studies by Tilgner et al. (2014) revealed a more stable stratification during this event with no large differences observed in the coefficient of divergence of the particles, suggesting that the possibility of entrainment of polluted air masses from above was rather low. These increased trace metals are often found from traffic emissions relating to car brake wear (Maenhaut et al., 2005) or from fuel combustion (Lee and Vonlehmd, 1973). The GB measurement site was close to the main road linking GB and Mt. Schmücke and could be influenced by traffic especially during weekends (period of this event) when more touristic activities are present in this region, thus suggesting that traffic emissions may have influenced these concentrations. A different trend was observed during the FCE 13.3 during which the total mass of the trace metals decreased. No significant changes in the shape of the size distribution of most elements were observed. The major elements observed were also Fe, Zn, and Pb. A similar trend was observed during FCE 22.1 with the trace metal concentration decreasing from GL to GB and the size distribution of these metals not changing significantly. Slight increases in Cr and Cu were observed in the coarse mode fraction at GB.

During most of the FCEs the total trace metal concentration dropped from GL to GB preserving the size distribution. An exception was observed during FCE 11.3 where a significant difference was not observed in the coarse mode fraction. Fe, Rb, Sr, Mn, and Ti were mostly found in the coarse mode while Pb, Zn, As, Se, Cr, and Ni were mostly found in the fine mode aerosol particles. Fe and Zn were the most deposited trace metals especially during FCE 1.1 and FCE 11.3. Although back trajectory analysis showed slight differences between the air mass origins during FCEs 1.1, 11.3, and 13.3, this difference was not strongly reflected in the trace metal distributions and no significant difference in the relative contribution of a particular metal was observed. Details on the likely sources of these trace metals will be further discussed in Sect. 3.3 below.

3.3 Correlation between trace metals and other aerosol chemical components

3.3.1 Levoglucosan

Figure 2 shows scatter plots of levoglucosan with potassium, zinc, lead, and arsenic in the particulate matter at the upwind (GL) and downwind (GB) stations in $PM_{1.2}$ particles. These elements showed good correlation with levoglucosan, both in $PM_{1.2}$ and $PM_{3.5}$ particles. The p values of these plots were less than 0.05. Nevertheless, since these correlations are based on statistically few data points, their values are used to mainly indicate possible trends between these components. In some cases these trends match observations elsewhere. Alongside potassium, levoglucosan is known (Schkolnik and Rudich, 2006; Simoneit et al., 1999; Iinuma et al., 2007) to be a good tracer for particles originating from biomass burning. The correlations with levoglucosan could be indicative of a common source, such as biomass burning. Zn amongst other elements has been observed in biomass combustion emissions (Fine et al., 2004) and although it is not largely accumulated in plants as has been observed by Schmidl et al. (2008), plumes of biomass burning as well as the applied

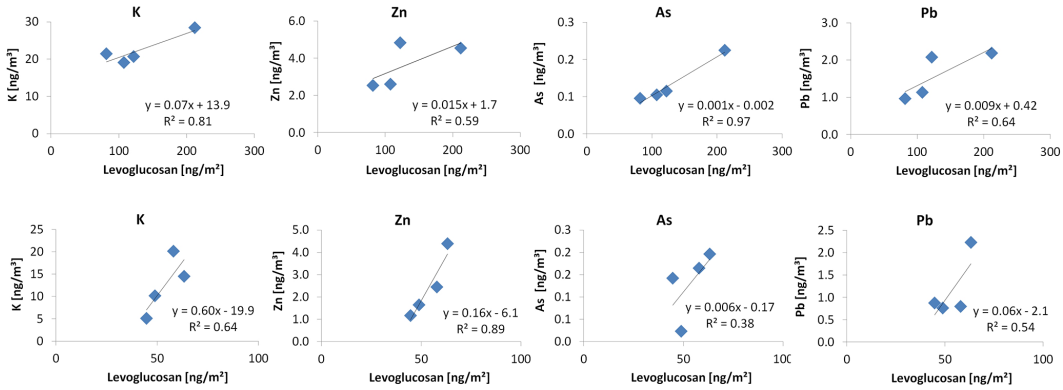

Figure 2. Scatter plots of levoglucosan, a biomass burning tracer, and K, Zn, As and Pb, in $PM_{1.2}$ particulate matter at **(a)** upwind GL and **(b)** downwind GB stations during HCCT2010.

Table 2. Correlation coefficients (r^2) between levoglucosan and Zn, K, Pb, Fe, and As before (GL) and after (GB) air mass parcel passed through the cloud with p values less than 5 %.

$PM_{1.2}$		Zn	K	Pb	AS	Fe	Mn
Levoglucosan	GL	0.59	0.81	0.64	0.97	0.95	0.70
	GB	0.88	0.64	0.54	0.38	0.55	0.66

fuel (Boman et al., 2006) or emissions from the walls of the combustion chambers can influence their concentrations in the atmosphere. These correlations, however, may also be simply due to changes in similar meteorological conditions.

Table 2 shows the correlation coefficients of levoglucosan and other trace metals in $PM_{1.2}$ particles at both valley stations before and after the passage of air mass through the cloud. Positive correlations were also observed for Mn and Fe with levoglucosan at Goldlauter on the upwind side. However, changes in the correlations were observed as the air mass passed through the cloud at the mountain station before arriving at Gehlberg. As shown in Table 2, the correlations of K, Fe, and As with levoglucosan became weaker suggesting that deposition of levoglucosan and particles containing such metals during the air mass transport over the mountain to GB may have significantly affected the state at which these components were present at GL. Levoglucosan is a water-soluble compound that can dissolve in cloud water and may also be lost from particles, aqueous reaction in cloud drops, or deposition of the cloud droplets. Such losses may account for the lower (about 40 %) concentration of levoglucosan observed at the downwind stations as depicted in Fig. 2b and the observed change in the correlation with the trace metals observed in Table 2. Similarly, trace metals can also be deposited during their transport.

The combination of these losses may lead to differences in the correlations observed between the upwind and downwind stations. In principle, no differences in this tendency were observed for the coarse and fine mode concentrations of these components, indicating that the fine mode aerosols carried most of the observed levoglucosan. Similar observation has been reported elsewhere (Herckes et al., 2006).

3.3.2 Elemental and organic carbon

Elemental carbon (EC) is often considered as soot particles that are emitted from diesel engines, or from other combustion processes as well as from industrial emissions, while organic carbon (OC) has both anthropogenic and biogenic sources (Herrmann et al., 2006; Saarikoski et al., 2008). In rural areas such as GL and GB, EC could originate from combustion processes or long-range transport from industrial and urban regions. Figures 3 and 4 show scatter plots of Ti, Mn, and Fe against OC as well as Pb, As, and Zn against EC at the upwind stations. The scatter plots reveal good correlation between these components in $PM_{3.5}$ particles. Good correlations were also observed for selenium with EC as well as Zn with OC. As explained above changes in meteorological conditions may lead to correlations between aerosol components. However, it has been observed elsewhere that these components could originate from sources such as fossil fuel or coal combustion (Hashimoto et al., 1970; Pacyna, 1984; Zhang et al., 2014), long-range transport, or traffic emissions relating to tire or brake wear (Handler et al., 2008).

EC correlation with Pb, Se, As, and Zn remained stable after passage of air masses through the cloud, implying that the Se-, Pb-, or As-containing material might have not been strongly deposited or lost during their transport through the cloud, or the deposition of these metals and EC were similar. Apparently, these elements are mostly present in particles in the fine mode. OC also showed good correlation with Fe after passage of air mass through the cloud but poor correlation with Ti and Mn. The poor correlation after passage

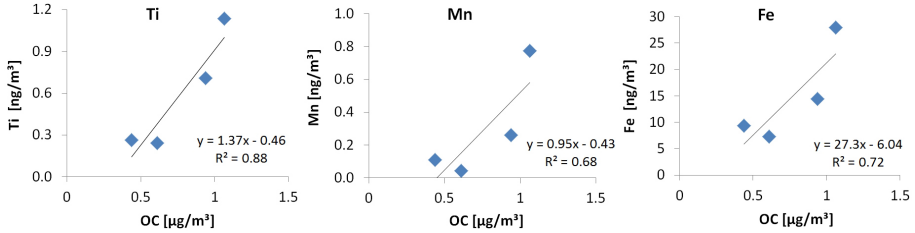

Figure 3. $PM_{3.5}$ scatter plots of Ti, Mn, and Fe against OC at the upwind stations.

of air mass through the cloud as already explained above is probably related to preferential loss via wet or dry deposition of Ti or Mn as well as of OC / EC-containing particles.

3.3.3 Other correlations

At the upwind station, oxalate showed good correlation with iron ($r^2 = 0.69$). This correlation between oxalate and iron as also observed above for iron and organic carbon indicates that the studied aerosols could be aged aerosols from sources such as biomass burning or even crustal sources especially for the coarse mode fractions. This correlation did not change significantly after the passage of the air parcel through the cloud especially during the FCEs. Despite the fact that the photolysis of iron oxalate complexes in aqueous media is known (Weller et al., 2013) to lead to the destruction of oxalate, which may indirectly lead to a poor correlation between iron and oxalate after the air mass passes through the cloud, and also particulate matter loss due to droplet deposition, a significant change of the correlation was not observed. However, this could also be due to the fact that most of the cloud events were observed in the evening hours where photochemical processes such as photolysis are not significant.

3.4 Enrichment factor analysis

Enrichment factor (EF) analysis was performed on $PM_{3.5}$ aerosol trace metals to evaluate the contribution of crustal material to the aerosol trace metals obtained at the valley stations. The evaluation was done using upper continental crust composition with Ti chosen as a marker for crustal material (Wedepohl, 1995). The EF of an element Z in the aerosol with respect to its composition in the crust is given as

$$\mathrm{EF} = \frac{(Z/\mathrm{Ti})_{\mathrm{Aerosol}}}{(Z/\mathrm{Ti})_{\mathrm{Crust}}}.$$

An enrichment factor above 10 is considered as a significant enrichment of the element and below 0.70 as a strong depletion in comparison to the composition of the reference source. Enrichment factors between 0.70 and 2 are considered to be similar and within the error range of the reference source, implying that the elements with such factors might have originated from a similar source while enrichment factors between 2 and 10 are considered to be moderately enriched. Figure 5 shows the size-resolved enrichment factors with respect to Ti for the measured elements of the various impactor stages at the valley stations GL and GB during HCCT 2010. The values are average enrichment factor values for the FCEs and the standard deviation plotted as error bars to indicate the variability of the values for each element at the various stations. As shown in Fig. 5, the enrichment factors decreased with particle size with lower enrichment observed for the coarse mode fraction (such as stage 4) in comparison to the fine mode fraction (stages 1 and 2). In principle, no significant difference especially for the fine mode particles was observed between the enrichment factors of the elements at the upwind and downwind stations, implying that the aerosol–cloud interactions did not lead to heavy loss of only a particular element with respect to Ti. Slight differences were observed with slightly higher enrichment factors observed at the downwind stations in comparison to the upwind station in the coarse mode fraction. This slight increase could be as a result of preferential loss through, for example, deposition processes of crustal material containing Ti which is more present in the coarse mode than in the fine mode.

Despite these changes, clear trends with increasing enrichment factors from Rb to Se could be observed. Trace metals were identified and grouped according to their similar EF. One group of trace metals including Mn, Fe, Co, Rb, and Sr showed little to no enrichment at all the stages at both the upwind and downwind stations with EF < 10 indicating that their occurrences were predominantly of crustal origin. Slightly elevated enrichment factors observed for Fe and Mn in fine mode fraction stages 2 and 3 are likely related to the emission of these elements from other sources such as coal combustion as well as biomass burning. The good correlations observed above between iron and oxalate or levoglucosan as well as between Mn, Fe, and organic carbon is a further indication of the likely influence of these combustion sources. The second group of elements includes V, Cr, and Ni. These elements showed high enrichment at all the stages and at both stations indicating they were of anthropogenic origin. Such metals are known to originate from fuel oil or coal combustion (Lee and Vonlehmd, 1973). The last group of trace metals including Cu, Zn, AS, Pb, and Se showed very high enrichment factors with values higher than 1000 in the fine mode. The very high enrichment is also indicative of their anthropogenic origins. Cu and Zn are known to

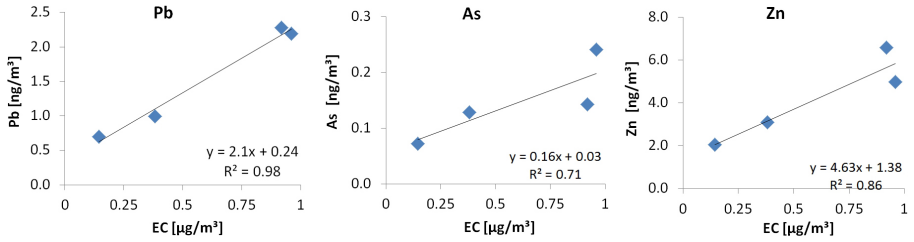

Figure 4. $PM_{3.5}$ scatter plots of Pb, As, Zn against EC at the upwind stations.

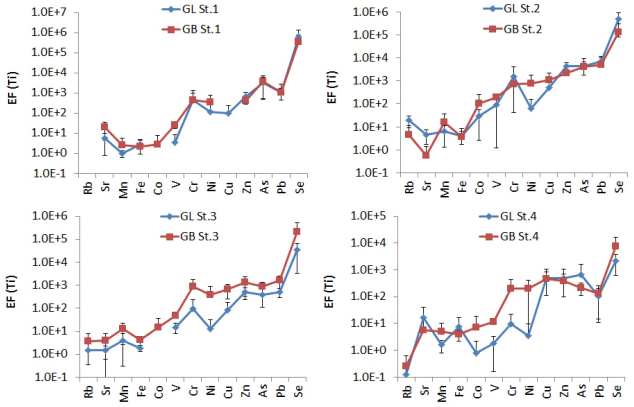

Figure 5. Size-resolved enrichment factor analysis of aerosol trace metals at the valley stations. Plotted values are averaged over all FCEs with their respective standard deviations plotted as error bars.

be emitted from exhaust gas (Pakkanen et al., 2003) and also car brake linings and tire wear in urban aerosols (Maenhaut et al., 2005). Zn, As, Se, and Pb have been observed from high-temperature combustion processes such as coal combustion or waste incineration processes as well as from non-metallurgic industrial processes (Belis et al., 2013; Minguillon et al., 2007; Pacyna et al., 2007). The correlations observed between Zn, As, Pb, and elemental carbon further support the likely influence of such sources. These metals were also strongly enriched in the fine fraction of the aerosol particles and could have also originated from long-range transport due to the long atmospheric lifetimes of fine particles. Back trajectory analysis of the air masses during these four events showed that the air masses crossed populated and industrial regions in Germany and France prior to their arrival at the measurement site.

3.5 Cloud water trace metal concentration

The average concentrations and the range of the various metal concentrations observed at Mt. Schmücke are presented in Table 3. Reported concentrations from previous FEBUKO experiment performed at the same location in 2002 and also reported concentrations from fog and cloud measurements done at other mountain sites in the world are also presented. For comparison of the cloud data with the valley stations, and for the understanding of the changes from sample to sample, and to obtain the equivalent air loading, the variation of the liquid water content (LWC), which alters dilution of solutes in the cloud water, was removed by multiplying the cloud water aqueous concentration with the LWC.

Trace metal concentrations decreased from Ti, Mn, Cr, to Co in cloud water. The average Ti concentration was observed at 9.8 $\mu g\,L^{-1}$ (2.6 $ng\,m^{-3}$) while for Mn, Cr, and Co, average concentrations of 5.59 $\mu g\,L^{-1}$ (1.54 $ng\,m^{-3}$), 5.54 $\mu g\,L^{-1}$ (1.5 $ng\,m^{-3}$), and 0.46 $\mu g\,L^{-1}$ (0.13 $ng\,m^{-3}$), respectively, were observed. The average concentrations of Sr, Pb, and Se ranged between 1.38 and 2.45 $\mu g\,L^{-1}$ while for V, As, Rb, and Co, their concentrations were $< 1\,\mu g\,L^{-1}$. Compared to previous FEBUKO experiments, apart from Cr, the average trace metal concentrations observed during HCCT were lower for most of the elements but their concentration ranges were similar to those observed during FEBUKO. The lower average concentrations might be due to reduction in particulate matter emissions over the time period of these studies in this area. Pb concentrations during HCCT were lower than those reported at Mt. Brocken (Plessow et al., 2001) and at Fichtelgebirge (Wrzesinsky and Klemm, 2000) but were higher than those reported in fogs at rural regions in Pennsylvania (Straub et al., 2012) and in marine clouds (Vong et al., 1997; Wang et al., 2014). Rb, Sr, and As concentrations were similar to those observed at Mt. Brocken; however, As values were lower than those observed at Fichtelgebirge (Wrzesinsky and Klemm, 2000). Mn and Se concentrations were within a similar order of magnitude as those reported at Mt. Brocken, Fichtelgebirge, and in marine clouds. However, the concentrations were far lower than those reported in cloud water at Mt. Tai, China (Guo et al., 2012; Liu et al., 2012). Lower concentrations than those observed in this study have also been reported by Wang et al. (2014) at higher elevated stratocumulus clouds collected via measurements using aircraft in California. The differences in these concentrations are related to differences in location and source influence, hence, differences in air mass origin and in the cloud droplet composition.

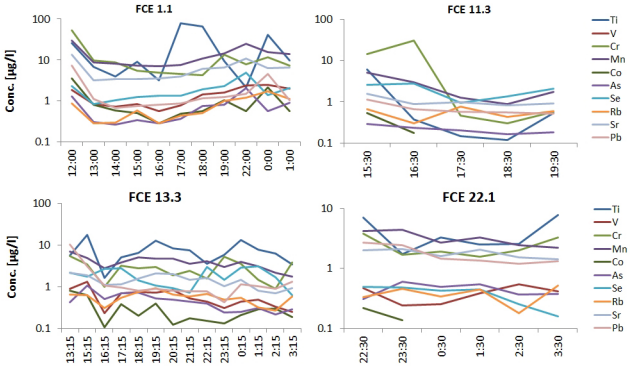

Figure 6. Trends in total trace metal cloud water concentrations during selected full cloud events: FCE 1.1: 14–15 September 2010, FCE 11.3: 2 October 2010, FCE 13.3: 6–7 October 2010, and FCE 22.1: 19–20 October 2010.

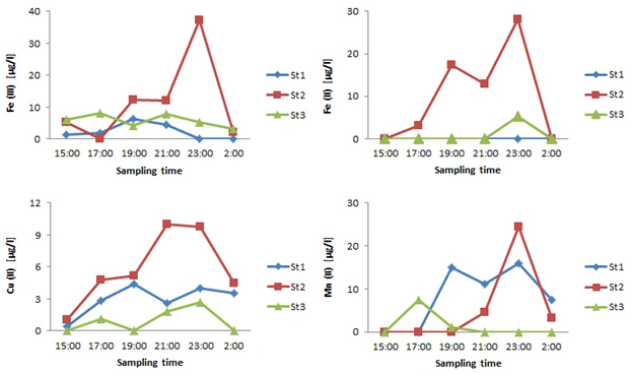

Figure 7. Temporal variation of size-resolved soluble transition metal ions, Fe(III), Fe(II), Cu(II), and Mn(II) in cloud water on 14–15 September 2010 during FCE 1.1. The nominal stage cutoffs were 22, 16, and 4 µm for St. 1, St. 2, and St. 3, respectively.

3.5.1 Temporal variation of trace metals during selected FCEs

Figure 6 shows the temporal variation of the trace metals during the four FCEs and the variations between the cloud events. Often, higher trace metal concentrations were observed during the first hours of the events and subsequently decreased during the course of the event. This trend was mostly observed during FCE 1.1 and FCE 11.3, while during FCE 1.1 very small differences were observed between the temporal variations of the metals. During FCE 1.1 the trace metal concentrations show uniform variation with slight increase in concentrations observed after 17:00. While As, Pb, Se, V, and Mn showed similar trends, Ti and Cr showed very different patterns. Similar trends were observed during FCEs 11.3, 13.3, and 22.1 for As, Pb, and Mn, respectively. Ti trends were unique throughout the FCEs. During FCE 13.3 and FCE 22.1, Co, V, and Cr showed similar temporal variations. The temporal variations in the trace metal concentrations are likely due to the temporal changes in the trace metal concentrations in the activated cloud condensation nuclei (CCN) and changes in air mass origin. The similar trend in the temporal variation of the trace metals is indicative of their similar origin. Ti is a good tracer for crustal sources while Pb and V are good tracers of anthropogenic activities. Thus, the origins of the trace metals were similar throughout most of the events and were of anthropogenic and crustal origins.

3.5.2 Size-resolved soluble metal ions

Soluble Fe(III), Fe(II), Cu(II), and Mn(II) were measured from 0.45 µm syringe filtered samples collected using a plastic three-stage CASCC collector with Teflon collection surfaces. However, because of low sampling amounts only the analyses during FCE 1.1 were successful. The size distribution and temporal variations of these ions are shown in Fig. 7. The nominal cloud water size cutoffs were 22, 16, and 4 µm for stages (St.) 1, 2, and 3, respectively. Fe(II) was mainly found on the second stage (size range: 16–22 µm) with concentrations of up to 28.2 µg L^{-1} meanwhile Fe(III) was found on all of the stages during the event with observed concentrations ranging up to 37.1 µg L^{-1}. The lowest concentration of Fe(III) was found in the larger droplets (stage 1). Soluble Cu(II) was concentrated in the first and second stages, likewise Mn(II). The Cu(II) concentrations ranged from 0.4 to 10.5 µg L^{-1} with higher concentrations observed on the second stage. Mn(II) concentrations varied from 1.1 to 24.5 µg L^{-1} with about 48 % present in the larger droplets (stage 1), which was different to the size distribution of the other measured TMIs.

Similar soluble trace metal concentrations have been reported in fogs (Straub et al., 2012) and cloud water (Li et al., 2013; Parazols et al., 2006; Hutchings et al., 2009) in other regions. The differences in the size distribution of these trace metals suggest that these TMIs might have had different source origins especially for Mn and Fe. Although Mn as well as Fe has high crustal abundance, both also have different anthropogenic sources such as waste incineration or metallurgical industries for Mn and fly ash for Fe. Fine mode iron can also be emitted from fuel combustion processes (Sholkovitz et al., 2012), which can thus explain its occurrence in this size fraction. Thus, the differences in the size distribution of these metal ions could be due to their source origins during this event or the differences in the efficiency of activation of the particles containing these metals. Fe(II) was observed mostly during evening hours during which photochemical processes are expected to be low due to lower solar radiation. This indicates that the observed nighttime Fe(II) concentrations were not directly related to photochemical processes. Fe(III) is known to be the most stable form of iron, but it can be reduced to Fe(II) via HO_x radicals or Cu(I). The production of HO_x radicals is predomi-

Table 3. Mean and range of trace metal concentrations in cloud water at Mt. Schmücke during HCCT 2010.

	HCCT		[ng m^{-3}]		Ref. A		Ref. B		Ref. C		Ref. D	Ref. E		Ref. F	
	Mean	Range	Mean	Range	Mean	Range	Median	Range	Mean	Range	Mean	Mean	Range	Mean	Range
Ti	9.18	0.1–79.1	2.60	0.01–24.1			2.3	< 1–466							
V	0.71	0.1–2.5	0.19	0.03–0.5		0–26	1.8	0.4–15.0			1.3			1.3	0.5–1.4
Cr	5.54	0.3–52	1.54	0.11–14	0.52	< 9.3	< 0.3	< 0.3–9.0				1.1	< 3.6		
Mn	5.59	0.1–30.1	1.50	0.01–8.1		4.8–133	7.8	1.0–158	66.3	< 1645	1.1			4.4	3.2–14.0
Co	0.46	0.1–3.5	0.13	0.01–0.9			0.08	< 0.02–2.1							
Se	1.38	0.1–4.9	0.42	0.01–1.7		< 9.6			13.2	< 99.9		4.7	1.1–11.5		
Pb	1.40	0.3–10.5	0.38	0.04–2	4.2	2.8–63	11	1.97–84.0			0.5	27.6	3.4–61.4	0.6	0.4–2.3
As	0.63	0.2–4.1	0.15	0.03–0.4			0.4	0.4–6.6				3.1	< 13.2		
Rb	0.57	0.1–1.7	0.16	0.01–0.3			< 1	< 1–6							
Sr	2.45	0.2–13.5	0.66	0.02–3.6			2.3	0.1–68.7							

Concentrations are in µg L^{-1} unless otherwise mentioned. Ref. A – Rüd (2003), Mt. Schmücke; Ref. B – Plessow et al. (2001), Mt. Brocken; Ref. C – Guo et al. (2012), Mt. Tai; Ref. D – Vong et al. (1997), marine clouds; Ref. E – Wrzesinsky and Klemm (2000), Fichtelgebirge; Ref. F – Straub et al. (2012), fog in rural Pennsylvania.

nantly photochemically driven. Their reactions with Fe(III) are, therefore expected to be faster in the presence of UV light such as during daytime; meanwhile, the reduction of Fe(III) to Fe(II) via Cu(I) is not directly limited by solar radiation and thus could be dominant at night (Deguillaume et al., 2004).

Due to the fast oxidation of Cu(I) to Cu(II), it is easier to measure Cu(II) than Cu(I). During FCE 1.1, Cu(II) was successfully measured with results revealing comparable concentrations as those reported elsewhere (Deguillaume et al., 2005; Li et al., 2013; Hutchings et al., 2009). The Cu(II) temporal variation is also shown in Fig. 7. The observed Cu(II) concentration in the same size fraction as soluble iron indicates that the Fe(II) at night could have been related to aqueous-phase reductions of Fe(III) to Fe(II) by Cu(I) species. Fe(III) catalyzed oxidation of sulfur (IV) has been suggested to be another important source of Fe(II) in cloud water during nighttime (Schwanz et al., 1998; Millero et al., 1995). However, with no data available on sulfur (IV) measurements during FCE 1.1, conclusions about the contribution of this pathway cannot be made. Anthropogenic sources of Fe in the environment, e.g., in fly ash, biomass burning emissions and other combustion sources, have been found to contain considerable concentration of Fe(II) (Trapp et al., 2010). This suggests that, although aqueous-phase reduction processes could have contributed to the observed nighttime Fe(II) concentrations, the source of the aerosol cannot be neglected. Nighttime concentrations of Fe(II) have also been observed in different studies, but no unique reason for their occurrence has been presented yet (Schwanz et al., 1998; Kotronarou and Sigg, 1993; Siefert et al., 1998; Parazols et al., 2006). The variation of the soluble trace metal concentrations with cloud drop size suggests that the metal-catalyzed oxidation of S(IV) may be strongly drop size dependent since the concentrations of TMIs influence the in-cloud S(IV) oxidation rates (Rao and Collett, 1998).

3.6 Comparison between trace metal concentrations in cloud water and in particles

3.6.1 Total trace metal concentration

As shown in Tables 1 and 3, Mn, Rb, and Ti in cloud water were higher than at the valley stations. However, although the average values for Mn and Ti were higher in cloud water as compared to those from the valley stations, the concentration ranges were similar. One reason for the observed difference in the Mn, Ti, and Rb concentrations could have been the analyzed particle size from the impactor samples collected from the valley stations. Mn, Ti, and Rb are often of crustal origin and also often found in the coarse aerosol fraction. As explained above, the aerosol trace metal analysis was performed only on $PM_{3.5}$ particles. Thus, the difference in the sampled particle sizes may explain the observed difference. For other trace metals such as V, Co, Se, As, and Sr, only small differences were observed with slightly lower concentrations observed in the cloud water in comparison to those at the valley stations. The average Pb and Cr concentrations were also lower in cloud water as compared to the concentrations at the valley stations. The observed differences between the cloud water and aerosol particle concentrations are also related to the strong variation of the trace metal concentrations during the FCEs due to their varying sources as well as the variation in the activation of the particles to suitable CCN.

3.6.2 Soluble trace metal concentration

Soluble aerosol trace metal concentrations were measured from 0.45 µm syringe filtrates obtained from DI water extracts of PM_{10} bulk samples, and the concentrations were compared with those obtained from filtered cloud water to find out if there were significant changes in the soluble trace metal concentration after the passage of the air mass through the cloud. Table 4 summarizes the soluble metal concentrations during selected FCEs. Due to the observed high blanks of Fe, Zn, Cu, and Mn in bulk cloud water samples, their values were not discussed except during FCE 1.1 whereby

Table 4. PM_{10}-soluble aerosol trace metal content at the upwind station Goldlauter (GL), downwind station Gehlberg (GB), and soluble trace metals in cloud water at Mt. Schmücke (SM) during four FCEs.

Events		Ti	V	Cr	Mn	Fe	Ni	Cu	Zn	As	Se	Rb	Sr	Pb
	GL	0.27	0.19	0.37	1.01	1.81	0.69	1.77	13.63	0.80	0.32	0.21	0.81	0.95
FCE 1.1	SM	0.15	0.17	0.93	**0.57**	**1.69**	**0.14**	**1.35**		0.08	0.32	0.07	0.89	0.48
	GB	0.09	0.24	0.46	0.84	–	0.39	1.34	13.68	0.62	0.32	0.11	0.72	1.53
	GL	0.40	0.00	0.25	0.19	1.20	0.18	0.37	7.38	0.39	0.17	0.19	0.25	0.26
FCE11.3	SM	0.11	0.00	0.24	0.38					0.02	0.51	0.11	0.35	0.34
	GB	0.28	0.00	0.47	0.34	0.64	0.22	–	9.86	0.60	0.71	0.08	0.74	0.39
	GL	0.10	0.11	0.28	0.70	5.82	0.70	3.23	5.28	0.22	1.09	0.16	0.33	0.88
FCE13.3	SM	0.41	0.16	0.23	0.64					0.08	0.64	0.16	0.40	0.58
	GB	–	0.06	0.45	0.42	3.86	0.24	0.73	4.08	0.19	0.63	0.10	0.16	0.97
	GL	0.12	0.00	1.19	0.30	1.14	0.43	0.54	3.48	0.30	0.12	0.12	0.30	0.36
FCE22.1	SM	0.31	0.10	0.29	0.61					0.10	0.10	0.10	0.61	0.98
	GB	0.38	0.12	0.20	0.16	1.44	0.10	–	2.36	0.08	0.06	0.06	0.22	0.29

Concentrations are in ng m^{-3}.

the values of the sized-resolved analysis presented above are included (in bold). The size-resolved data were converted to bulk concentrations by multiplying the volume-weighted mean size-resolved concentrations with the bulk LWC. As shown in Table 4, during FCE 1.1 no significant change in the soluble content of the trace metals was observed before and after the cloud. Mn, Cu, Ni, and Zn, as well as As, Se, Sr, V, and Cr concentrations were of the same order of magnitude while only slight increases were registered for Pb concentrations. Cu, Mn, and Fe concentrations were within the same order of magnitude as those at the valley stations, suggesting that there might have been no significant in-cloud processing of the particles containing these metals that affected trace metal solubility. During FCE 11.3 small increases in the soluble concentration of Cr, Mn, Ni, Cu, Zn, As, and Pb were observed between Goldlauter and Gehlberg. However, during FCE 13.3 the soluble content decreased from Goldlauter to Gehlberg for elements such as V, Mn, Fe, Ni, Cu, Zn, As, Se, Rb, and Sr while a slight increase could only be observed for Ti and Cr. Similarly, during FCE 22.1 an increase in soluble content was observed for Ti, V, Fe, and Cu, while a decrease was observed for Cr, Mn, Ni, Zn, As, Se, Rb, Sr, and Pb.

Although it is known that cloud processes enhance the solubility of trace metals, especially for elements such as Fe via acid dissolution or complexation with organic acids such as oxalic acid, no clear trend and significant difference was observed between the upwind station (GL) and the downwind station (GB) soluble iron concentrations. Since most of the FCEs were observed in the evening period, the possibilities for photochemical processes to occur were limited. As with iron, no clear trend in the variation of the soluble trace metal concentrations was observed for the other metal ions during all the FCEs. The variation in the observed concentrations during the different FCEs is also related to influences in air mass origin and the loss due to preferential deposition of larger or more efficiently cloud-scavenged particles.

4 Summary

The characterization of trace metals in size-resolved and bulk aerosol particles at the valley upwind (Goldlauter, GL) and downwind (Gehlberg, GB) stations as well as in cloud water at Mt. Schmücke during four cloud events during HCCT has been presented. The concentrations of the 14 investigated trace metals showed variations between the cloud events with Fe and Zn being the most abundant observed trace metals in the aerosol. The most deposited trace metals between the upwind and downwind stations were also Fe and Zn. Aerosol particle trace metal concentrations were lower than those observed in the same region during the FEBUKO field experiments about 9 years ago. The decrease in metal concentrations could be related to decreases in emission as well as differences in the PM size fraction analyzed ($PM_{3.5}$ vs. PM_{10}). Aerosol and cloud trace metal concentrations observed in this study were within a similar range to those observed in other rural regions in Europe. Strong changes in aerosol particle chemical properties were observed as particles passed through clouds with changes in the correlation between some chemical components observed. Trace metals such as Zn, Pb, Fe, Mn, and Ti showed good correlation with levoglucosan, oxalate, and organic and elementary carbon suggesting their similar source origins. In addition to correlation analysis, enrichment factor analysis showed that trace metals during HCCT were of various origins, including crustal, biomass burning, coal combustion, long-range transport, and traffic sources. Soluble aerosol trace metal concentrations did not show strong variations after aerosol–cloud interaction.

However, size-resolved soluble trace metal concentrations in cloud water showed a non-uniform distribution of Fe, Cu, and Mn across the drop sizes with Cu and Fe mainly found in drop sizes between 16 and 22 µm and Mn in drop sizes greater than 22 µm. Such variations suggest that TMI catalytic processes such as TMI enhanced oxidation of S(IV) may be drop size dependent. Soluble iron was mainly found in its Fe(III) state. Strong temporal variation was observed in the soluble Fe concentrations with Fe(II) dominating the soluble iron concentrations during some episodes. In contrast to other studies, Fe(II) was mostly observed in the evening hours implying its presence in cloud water was not directly related to photochemical processes.

Acknowledgements. The authors acknowledge the support of several TROPOS staff members during cloud water sampling and aerosol sampling, the German Federal Environmental Agency (UBA) for their support and cooperation at Schmücke field site and the administrations of the villages Suhl-Goldlauter and Gehlberg for their help. HCCT-2010 was partially funded by the German Research Foundation (DFG) under contract HE 3086/15-1. Partial additional support for Colorado State University was provided by the US National Science Foundation (AGS-846 0711102 and AGS-1050052).

Edited by: C. George

References

Aldabe, J., Elustondo, D., Santamaria, C., Lasheras, E., Pandolfi, M., Alastuey, A., Querol, X., and Santamaria, J. M.: Chemical characterisation and source apportionment of $PM_{2.5}$ and PM_{10} at rural, urban and traffic sites in Navarra (North of Spain), Atmos. Res., 102, 191–205, doi:10.1016/j.atmosres.2011.07.003, 2011.

Allen, A. G., Nemitz, E., Shi, J. P., Harrison, R. M., and Greenwood, J. C.: Size distributions of trace metals in atmospheric aerosols in the United Kingdom, Atmos. Environ., 35, 4581–4591, 2001.

Belis, C. A., Karagulian, F., Larsen, B. R., and Hopke, P. K.: Critical review and meta-analysis of ambient particulate matter source apportionment using receptor models in Europe, Atmos. Environ., 69, 94–108, doi:10.1016/j.atmosenv.2012.11.009, 2013.

Boman, C., Öhman, M., and Nordin, A.: Trace Element Enrichment and Behavior in Wood Pellet Production and Combustion Processes, Energ. Fuel., 20, 993–1000, doi:10.1021/ef050375b, 2006.

Bruggemann, E., Gnauk, T., Mertes, S., Acker, K., Auel, R., Wieprecht, W., Moller, D., Collett, J. L., Chang, H., Galgon, D., Chemnitzer, R., Rud, C., Junek, R., Wiedensohler, W., and Herrmann, H.: Schmucke hill cap cloud and valley stations aerosol characterisation during FEBUKO (I): Particle size distribution, mass, and main components, Atmos. Environ., 39, 4291–4303, doi:10.1016/j.atmosenv.2005.02.013, 2005.

Burkhard, E. G., Mehmood, G., and Husain, L.: Determination of Trace-Elements in Cloud Water and Aerosols Using Instrumental Neutron-Activation Analysis and Hydride Generation with Atomic-Absorption Spectrometry, J. Radioan. Nucl. Ch. Ar., 161, 101–112, doi:10.1007/Bf02034884, 1992.

Cini, R., Prodi, F., Santachiara, G., Porcu, F., Bellandi, S., Stortini, A. M., Oppo, C., Udisti, R., and Pantani, F.: Chemical characterization of cloud episodes at a ridge site in Tuscan Appennines, Italy, Atmos. Res., 61, 311–334, doi:10.1016/S0169-8095(01)00139-9, 2002.

Clarke, A. G. and Radojevic, M.: Oxidation of SO_2 in Rainwater and Its Role in Acid-Rain Chemistry, Atmos. Environ., 21, 1115–1123, doi:10.1016/0004-6981(87)90238-1, 1987.

Deguillaume, A. M., Marie, O., Carde, A., Mourey, F., Rouveau, M., Faure, P., Schlemmer, B., and Touratier, S.: Long-term evaluation of practices in surgical antibiotic prophylaxis at Saint Louis Hospital, Int. J. Antimicrob. Ag., 24, S226–S226, 2004.

Deguillaume, L., Leriche, M., Desboeufs, K., Mailhot, G., George, C., and Chaumerliac, N.: Transition metals in atmospheric liquid phases: Sources, reactivity, and sensitive parameters, Chem. Rev., 105, 3388–3431, doi:10.1021/Cr040649c, 2005.

Demoz, B. B., Collett, J. L., and Daube, B. C.: On the Caltech Active Strand Cloudwater Collectors, Atmos. Res., 41, 47–62, doi:10.1016/0169-8095(95)00044-5, 1996.

Dongarra, G., Manno, E., Varrica, D., Lombardo, M., and Vultaggio, M.: Study on ambient concentrations of PM_{10}, $PM_{10\text{-}2.5}$, $PM_{2.5}$ and gaseous pollutants. Trace elements and chemical speciation of atmospheric particulates, Atmos. Environ., 44, 5244–5257, doi:10.1016/j.atmosenv.2010.08.041, 2010.

Fine, P. M., Cass, G. R., and Simoneit, B. R. T.: Chemical characterization of fine particle emissions from the wood stove combustion of prevalent United States tree species, Environ. Eng. Sci., 21, 705–721, doi:10.1089/ees.2004.21.705, 2004.

Fomba, K. W., Müller, K., van Pinxteren, D., and Herrmann, H.: Aerosol size-resolved trace metal composition in remote northern tropical Atlantic marine environment: case study Cape Verde islands, Atmos. Chem. Phys., 13, 4801–4814, doi:10.5194/acp-13-4801-2013, 2013.

Guo, J., Wang, Y., Shen, X. H., Wang, Z., Lee, T., Wang, X. F., Li, P. H., Sun, M. H., Collett, J. L., Wang, W. X., and Wang, T.: Characterization of cloud water chemistry at Mount Tai, China: Seasonal variation, anthropogenic impact, and cloud processing, Atmos. Environ., 60, 467–476, doi:10.1016/j.atmosenv.2012.07.016, 2012.

Handler, M., Puls, C., Zbiral, J., Marr, I., Puxbaum, H., and Limbeck, A.: Size and composition of particulate emissions from motor vehicles in the Kaisermuhlen-Tunnel, Vienna, Atmos. Environ., 42, 2173–2186, doi:10.1016/j.atmosenv.2007.11.054, 2008.

Harris, E., Sinha, B., van Pinxteren, D., Tilgner, A., Fomba, K. W., Schneider, J., Roth, A., Gnauk, T., Fahlbusch, B., Mertes, S., Lee, T., Collett, J., Foley, S., Borrmann, S., Hoppe, P., and Herrmann, H.: Enhanced Role of Transition Metal Ion Catalysis During In-Cloud Oxidation of SO_2, Science, 340, 727–730, doi:10.1126/science.1230911, 2013.

Hashimoto, Y., Hwang, J. Y., and Yanagisa, S.: Possible Source of Atmospheric Pollution of Selenium, Environ. Sci. Technol., 4, 157–158, doi:10.1021/Es60037a002, 1970.

Herckes, P., Engling, G., Kreidenweis, S. M., and Collett, J. L.: Particle size distributions of organic aerosol constituents during the 2002 Yosemite Aerosol Characterization Study, Environ. Sci. Technol., 40, 4554–4562, doi:10.1021/Es0515396, 2006.

Herrmann, H., Wolke, R., Muller, K., Bruggemann, E., Gnauk, T., Barzaghi, P., Mertes, S., Lehmann, K., Massling, A., Birmili,

W., Wiedensohler, A., Wierprecht, W., Acker, K., Jaeschke, W., Kramberger, H., Svrcina, B., Bachmann, K., Collett, J. L., Galgon, D., Schwirn, K., Nowak, A., van Pinxteren, D., Plewka, A., Chemnitzer, R., Rud, C., Hofmann, D., Tilgner, A., Diehl, K., Heinold, B., Hinneburg, D., Knoth, O., Sehili, A. M., Simmel, M., Wurzler, S., Majdik, Z., Mauersberger, G., and Muller, F.: FEBUKO and MODMEP: Field measurements and modelling of aerosol and cloud multiphase processes, Atmos. Environ., 39, 4169–4183, doi:10.1016/j.atmosenv.2005.02.004, 2005.

Herrmann, H., Bruggemann, E., Franck, U., Gnauk, T., Loschau, G., Muller, K., Plewka, A., and Spindler, G.: A source study of PM in saxony by size-segregated characterisation, J. Atmos. Chem., 55, 103–130, doi:10.1007/s10874-006-9029-7, 2006.

Hueglin, C., Gehrig, R., Baltensperger, U., Gysel, M., Monn, C., and Vonmont, H.: Chemical characterisation of $PM_{2.5}$, PM_{10} and coarse particles at urban, near-city and rural sites in Switzerland, Atmos. Environ., 39, 637–651, doi:10.1016/j.atmosenv.2004.10.027, 2005.

Hutchings, J. W., Robinson, M. S., McIlwraith, H., Kingston, J. T., and Herckes, P.: The Chemistry of Intercepted Clouds in Northern Arizona during the North American Monsoon Season, Water Air Soil Poll., 199, 191–202, doi:10.1007/s11270-008-9871-0, 2009.

Iinuma, Y., Bruggemann, E., Gnauk, T., Muller, K., Andreae, M. O., Helas, G., Parmar, R., and Herrmann, H.: Source characterization of biomass burning particles: The combustion of selected European conifers, African hardwood, savanna grass, and German and Indonesian peat, J. Geophys. Res.-Atmos., 112, D08209, doi:10.1029/2006jd007120, 2007.

Jacob, D. J. and Hoffmann, M. R.: A Dynamic-Model for the Production of H+, NO_3^-, and SO_4^{2-} in Urban Fog, J. Geophys. Res.-Oc. Atm., 88, 6611–6621, doi:10.1029/Jc088ic11p06611, 1983.

Kotronarou, A. and Sigg, L.: SO(2) Oxidation in Atmospheric Water – Role of Fe(Ii) and Effect of Ligands, Environ. Sci. Technol., 27, 2725–2735, doi:10.1021/Es00049a011, 1993.

Lee, R. E. and Vonlehmd, D. J.: Trace Metal Pollution in Environment, JAPCA J. Air Waste Ma., 23, 853–857, 1973.

Li, W. J., Wang, Y., Collett, J. L., Chen, J. M., Zhang, X. Y., Wang, Z. F., and Wang, W. X.: Microscopic Evaluation of Trace Metals in Cloud Droplets in an Acid Precipitation Region, Environ. Sci. Technol., 47, 4172–4180, doi:10.1021/Es304779t, 2013.

Liu, X.-H., Wai, K.-M., Wang, Y., Zhou, J., Li, P.-H., Guo, J., Xu, P.-J., and Wang, W.-X.: Evaluation of trace elements contamination in cloud/fog water at an elevated mountain site in Northern China, Chemosphere, 88, 531–541, doi:10.1016/j.chemosphere.2012.02.015, 2012.

Maenhaut, W., Raes, N., Chi, X. G., Cafmeyer, J., Wang, W., and Salma, I.: Chemical composition and mass closure for fine and coarse aerosols at a kerbside in Budapest, Hungary, in spring 2002, X-Ray Spectrom., 34, 290–296, doi:10.1002/Xrs.820, 2005.

Maenhaut, W., Raes, N., Chi, X. G., Cafmeyer, J., and Wang, W.: Chemical composition and mass closure for $PM_{2.5}$ and PM_{10} aerosols at K-puszta, Hungary, in summer 2006, X-Ray Spectrom., 37, 193–197, doi:10.1002/Xrs.1062, 2008.

Maenhaut, W., Nava, S., Lucarelli, F., Wang, W., Chi, X. G., and Kulmala, M.: Chemical composition, impact from biomass burning, and mass closure for PM(2.5) and PM(10) aerosols at Hyytiala, Finland, in summer 2007, X-Ray Spectrom., 40, 168–171, doi:10.1002/Xrs.1302, 2011.

Mancinelli, V., Decesari, S., Facchini, M. C., Fuzzi, S., and Mangani, F.: Partitioning of metals between the aqueous phase and suspended insoluble material in fog droplets, Ann. Chim.-Rome, 95, 275–290, doi:10.1002/adic.200590033, 2005.

Marenco, F., Bonasoni, P., Calzolari, F., Ceriani, M., Chiari, M., Cristofanelli, P., D'Alessandro, A., Fermo, P., Lucarelli, F., Mazzei, F., Nava, S., Piazzalunga, A., Prati, P., Valli, G., and Vecchi, R.: Characterization of atmospheric aerosols at Monte Cimone, Italy, during summer 2004: Source apportionment and transport mechanisms, J. Geophys. Res.-Atmos., 111, D24202, doi:10.1029/2006jd007145, 2006.

Masiol, M., Squizzato, S., Ceccato, D., and Pavoni, B.: The size distribution of chemical elements of atmospheric aerosol at a semi-rural coastal site in Venice (Italy). The role of atmospheric circulation, Chemosphere, 119, 400–406, doi:10.1016/j.chemosphere.2014.06.086, 2015.

Millero, F. J., Gonzalezdavila, M., and Santanacasiano, J. M.: Reduction of Fe(Iii) with Sulfite in Natural-Waters, J. Geophys. Res.-Atmos., 100, 7235–7244, doi:10.1029/94jd03111, 1995.

Minguillon, M. C., Querol, X., Alastuey, A., Monfort, E., Mantilla, E., Sanz, M. J., Sanz, F., Roig, A., Renau, A., Felis, C., Miro, J. V., and Artinano, B.: PM_{10} speciation and determination of air quality target levels. A case study in a highly industrialized area of Spain, Sci. Total. Environ., 372, 382–396, doi:10.1016/j.scitotenv.2006.10.023, 2007.

Moroni, B., Castellini, S., Crocchianti, S., Piazzalunga, A., Fermo, P., Scardazza, F., and Cappelletti, D.: Ground-based measurements of long-range transported aerosol at the rural regional background site of Monte Martano (Central Italy), Atmos. Res., 155, 26–36, doi:10.1016/j.atmosres.2014.11.021, 2015.

Müller, K., Lehmann, S., van Pinxteren, D., Gnauk, T., Niedermeier, N., Wiedensohler, A., and Herrmann, H.: Particle characterization at the Cape Verde atmospheric observatory during the 2007 RHaMBLe intensive, Atmos. Chem. Phys., 10, 2709–2721, doi:10.5194/acp-10-2709-2010, 2010.

Oktavia, B., Lim, L. W., and Takeuchi, T.: Simultaneous Determination of Fe(III) and Fe(II) Ions via Complexation with Salicylic Acid and 1,10-Phenanthroline in Microcolumn Ion Chromatography, Anal. Sci., 24, 1487–1492, doi:10.2116/analsci.24.1487, 2008.

Pacyna, E. G., Pacyna, J. M., Fudala, J., Strzelecka-Jastrzab, E., Hlawiczka, S., Panasiuk, D., Nitter, S., Pregger, T., Pfeiffer, H., and Friedrich, R.: Current and future emissions of selected heavy metals to the atmosphere from anthropogenic sources in Europe, Atmos. Environ., 41, 8557–8566, doi:10.1016/j.atmosenv.2007.07.040, 2007.

Pacyna, J. M.: Estimation of the Atmospheric Emissions of Trace-Elements from Anthropogenic Sources in Europe, Atmos. Environ., 18, 41–50, 1984.

Pakkanen, T. A., Kerminen, V. M., Loukkola, K., Hillamo, R. E., Aarnio, P., Koskentalo, T., and Maenhaut, W.: Size distributions of mass and chemical components in street-level and rooftop PM1 particles in Helsinki, Atmos. Environ., 37, 1673–1690, doi:10.1016/S1352-2310(03)00011-6, 2003.

Parazols, M., Marinoni, A., Amato, P., Abida, O., Laj, P., and Mailhot, G.: Speciation and role of iron in cloud droplets

at the puy de Dome station, J. Atmos. Chem., 54, 267–281, doi:10.1007/s10874-006-9026-x, 2006.

Plessow, K., Acker, K., Heinrichs, H., and Moller, D.: Time study of trace elements and major ions during two cloud events at the Mt. Brocken, Atmos. Environ., 35, 367–378, doi:10.1016/S1352-2310(00)00134-5, 2001.

Raja, S., Raghunathan, R., Yu, X. Y., Lee, T. Y., Chen, J., Kommalapati, R. R., Murugesan, K., Shen, X., Qingzhong, Y., Valsaraj, K. T., and Collett, J. L.: Fog chemistry in the Texas-Louisiana Gulf Coast corridor, Atmos. Environ., 42, 2048–2061, doi:10.1016/j.atmosenv.2007.12.004, 2008.

Rao, X. and Collett, J. L.: The drop size-dependence of iron and manganese concentrations in clouds and fogs: Implications for sulfate production, J. Atmos. Chem., 30, 273–289, doi:10.1023/A:1006044614291, 1998.

Rogula-Kozlowska, W., Klejnowski, K., Rogula-Kopiec, P., Osrodka, L., Krajny, E., Blaszczak, B., and Mathews, B.: Spatial and seasonal variability of the mass concentration and chemical composition of $PM_{2.5}$ in Poland, Air Qual. Atmos. Hlth., 7, 41–58, doi:10.1007/s11869-013-0222-y, 2014.

Rüd, C.: Bestimmung von Metallen in Aerosolpartikeln und Wolkenwasser mittels Atom-Absorptionsspektrometrie, Diplomarbeit, Universität Leipzig, 2003.

Saarikoski, S., Timonen, H., Saarnio, K., Aurela, M., Järvi, L., Keronen, P., Kerminen, V.-M., and Hillamo, R.: Sources of organic carbon in fine particulate matter in northern European urban air, Atmos. Chem. Phys., 8, 6281–6295, doi:10.5194/acp-8-6281-2008, 2008.

Schkolnik, G. and Rudich, Y.: Detection and quantification of levoglucosan in atmospheric aerosols: A review, Anal. Bioanal. Chem., 385, 26–33, doi:10.1007/s00216-005-0168-5, 2006.

Schmidl, C., Marr, I. L., Caseiro, A., Kotianová, P., Berner, A., Bauer, H., Kasper-Giebl, A., and Puxbaum, H.: Chemical characterisation of fine particle emissions from wood stove combustion of common woods growing in mid-European Alpine regions, Atmos. Environ., 42, 126–141, doi:10.1016/j.atmosenv.2007.09.028, 2008.

Schwanz, M., Warneck, P., Preiss, M., and Hoffmann, P.: Chemical speciation of iron in fog water, Contr. Atmos. Phys., 71, 131–143, 1998.

Sholkovitz, E. R., Sedwick, P. N., Church, T. M., Baker, A. R., and Powell, C. F.: Fractional solubility of aerosol iron: Synthesis of a global-scale data set, Geochim. Cosmochim. Ac., 89, 173–189, doi:10.1016/j.gca.2012.04.022, 2012.

Siefert, R. L., Johansen, A. M., Hoffmann, M. R., and Pehkonen, S. O.: Measurements of trace metal (Fe, Cu, Mn, Cr) oxidation states in fog and stratus clouds, J. Air Waste Manage., 48, 128–143, 1998.

Simoneit, B. R. T., Schauer, J. J., Nolte, C. G., Oros, D. R., Elias, V. O., Fraser, M. P., Rogge, W. F., and Cass, G. R.: Levoglucosan, a tracer for cellulose in biomass burning and atmospheric particles, Atmos. Environ., 33, 173–182, doi:10.1016/S1352-2310(98)00145-9, 1999.

Spindler, G., Gruner, A., Muller, K., Schlimper, S., and Herrmann, H.: Long-term size-segregated particle (PM_{10}, $PM_{2.5}$, PM_1) characterization study at Melpitz – influence of air mass inflow, weather conditions and season, J. Atmos. Chem., 70, 165–195, doi:10.1007/s10874-013-9263-8, 2013.

Spokes, L. J., Jickells, T. D., and Lim, B.: Solubilization of Aerosol Trace-Metals by Cloud Processing – a Laboratory Study, Geochim. Cosmochim. Ac., 58, 3281–3287, doi:10.1016/0016-7037(94)90056-6, 1994.

Straub, D. J., Hutchings, J. W., and Herckes, P.: Measurements of fog composition at a rural site, Atmos. Environ., 47, 195–205, doi:10.1016/j.atmosenv.2011.11.014, 2012.

Tilgner, A., Schöne, L., Bräuer, P., van Pinxteren, D., Hoffmann, E., Spindler, G., Styler, S. A., Mertes, S., Birmili, W., Otto, R., Merkel, M., Weinhold, K., Wiedensohler, A., Deneke, H., Schrödner, R., Wolke, R., Schneider, J., Haunold, W., Engel, A., Wéber, A., and Herrmann, H.: Comprehensive assessment of meteorological conditions and airflow connectivity during HCCT-2010, Atmos. Chem. Phys., 14, 9105–9128, doi:10.5194/acp-14-9105-2014, 2014.

Trapp, J. M., Millero, F. J., and Prospero, J. M.: Trends in the solubility of iron in dust-dominated aerosols in the equatorial Atlantic trade winds: Importance of iron speciation and sources, Geochem. Geophy. Geosys., 11, Q03014, doi:10.1029/2009gc002651, 2010.

Vlastelic, I., Suchorski, K., Sellegri, K., Colomb, A., Nauret, F., Bouvier, L., and Piro, J. L.: The trace metal signature of atmospheric aerosols sampled at a European regional background site (puy de Dme, France), J. Atmos. Chem., 71, 195–212, doi:10.1007/s10874-014-9290-0, 2014.

Vong, R. J., Baker, B. M., Brechtel, F. J., Collier, R. T., Harris, J. M., Kowalski, A. S., McDonald, N. C., and McInnes, L. M.: Ionic and trace element composition of cloud water collected on the Olympic Peninsula of Washington State, Atmos. Environ., 31, 1991–2001, doi:10.1016/S1352-2310(96)00337-8, 1997.

Wang, Z., Sorooshian, A., Prabhakar, G., Coggon, M. M., and Jonsson, H. H.: Impact of emissions from shipping, land, and the ocean on stratocumulus cloud water elemental composition during the 2011 E-PEACE field campaign, Atmos. Environ., 89, 570–580, doi:10.1016/j.atmosenv.2014.01.020, 2014.

Wedepohl, K. H.: The Composition of the Continental-Crust, Geochim. Cosmochim. Ac., 59, 1217–1232, 1995.

Weller, C., Horn, S., and Herrmann, H.: Effects of Fe(III)-concentration, speciation, excitation-wavelength and light intensity on the quantum yield of iron(III)-oxalato complex photolysis, J. Photoch. Photobio. A, 255, 41–49, doi:10.1016/j.jphotochem.2013.01.014, 2013.

Wrzesinsky, T. and Klemm, O.: Summertime fog chemistry at a mountainous site in central Europe, Atmos Environ, 34, 1487–1496, doi:10.1016/S1352-2310(99)00348-9, 2000.

Zhang, W., Tong, Y. D., Wang, H. H., Chen, L., Ou, L. B., Wang, X. J., Liu, G. H., and Zhu, Y.: Emission of Metals from Pelletized and Uncompressed Biomass Fuels Combustion in Rural Household Stoves in China, Sci. Rep.-UK, 4, 5611, doi:10.1038/Srep05611, 2014.

Zuo, Y. G. and Hoigne, J.: Photochemical Decomposition of Oxalic, Glyoxalic and Pyruvic-Acid Catalyzed by Iron in Atmospheric Waters, Atmos. Environ., 28, 1231–1239, 1994.